Neuropsychologia 47 (2009) 657–662

Contents lists available at ScienceDirect

Neuropsychologia

journal homepage: www.elsevier.com/locate/neuropsychologia

Hemodynamic changes in the infant cortex during the processing of featural and spatiotemporal information

Teresa Wilcox[a,*], Heather Bortfeld[a], Rebecca Woods[a], Eric Wruck[a], Jennifer Armstrong[a], David Boas[b]

[a] Texas A&M University, United States
[b] Anthinoula A. Martinos Center for Biomedical Imaging, Massachusetts General Hospital, Harvard Medical School, United States

ARTICLE INFO

Article history:
Received 22 April 2008
Received in revised form
12 November 2008
Accepted 14 November 2008
Available online 21 November 2008

Keywords:
Infants
Near-infrared spectroscopy
Object processing
Featural information
Spatiotemporal information

ABSTRACT

Over the last 20 years neuroscientists have learned a great deal about the ventral and dorsal object processing pathways in the adult brain, yet little is known about the functional development of these pathways. The present research assessed the extent to which different patterns of neural activation, as measured by changes in blood volume and oxygenation, are observed in infant visual and temporal cortex in response to events that involve processing of featural differences or spatiotemporal discontinuities. Infants aged 6.5 months were tested. Increased neural activation was observed in visual cortex in response to a featural-difference and a spatiotemporal-discontinuity event. In addition, increased neural activation was observed in temporal cortex in response to the featural-difference but not the spatiotemporal-discontinuity event. The outcome of this experiment reveals early functional specialization of temporal cortex and lays the foundation for future investigation of the maturation of object processing pathways in humans.

1. Introduction

Over the last 20 years a great deal of research has been conducted on the neural basis of object processing. Early studies conducted with non-human primates suggested that there are two main routes for visual object processing (De Yoe & Van Essen, 1988; Goodale & Milner, 1992; Livingstone & Hubel, 1988; Mishkin, Ungerleider, & Macko, 1983; Ungerleider & Mishkin, 1982). The *ventral* route originates from the parvocellular layers of the lateral geniculate nucleus (LGN) and projects from the primary visual cortex to the temporal cortex and mediates processing of visual features important for the recognition and identification of objects. The *dorsal* route originates from the magnocellular layers of the LGN and projects from the primary visual cortex to the parietal cortex and is important for the analysis of motion, depth, and location. More recent studies with non-human (Orban, Van Essen, & Fanduffel, 2004; Tootell, Tsao, & Vanduffel, 2003; Tsunoda, Yamane, Nishizaki, & Tanifuji, 2001; Wang, Tanifuji, & Tanaka, 1998; Wang, Tanaka, & Tanifuji, 1996) and human (Bly & Kosslyn, 1997; Grill-Spector, Kourtzi, & Kanwisher, 2001; Grill-Spector et al., 1998; Haxby et al., 1991; Kourtzi & Kanwisher, 2001; Kraut, Hart, Soher, & Gordon, 1997) primates, using more sophisticated neuroimaging techniques, provide converging evidence for the functional distinction between these two pathways.

Although we now have extensive information about the neural correlates of object processing in the adult, little is known about the functional development of these pathways. Research conducted with infant monkeys suggests that the temporal cortex undergoes significant structural and neurophysiological development early in life (Bachevalier, Brickson, Hagger, & Mishkin, 1990; Rodman, Skelly, & Gross, 1991; Webster, Ungerleider, & Bachevalier, 1991, 1995). Metabolic, neurophysiological, and neuroanatomical data obtained with human infants also reveals significant neural maturation during the first year (e.g., Braddick, Atkinson, & Wattam-Bell, 2003; Braddick & Atkinson, 2007; Chugani & Phelps, 1986; Conel, 1939–1967; De Haan & Nelson, 1999; Franceschini, Thaker, Themelis, Krishnamoorthy & Bortfeld, 2007; Gunn et al., 2002; Purpura, 1975). However, because there are a limited number of non-invasive techniques available to measure localized functional brain activation in infants, little is known about the functional consequences of neural maturation. Recent advances in optical imaging, including near-infrared spectroscopy (NIRS), now offer the opportunity to study functional activation in human infants.

In NIRS, near-infrared light is projected through the scalp and skull into the brain and the intensity of the light that is diffusely reflected is recorded. Typically, during cortical activation local concentrations of oxyhemoglobin (HbO_2) increase, whereas concentrations of deoxyhemoglobin (HbR) decrease (Hoshi & Tamura, 1993; Jasdzewski et al., 2003; Obrig et al., 1996; Strangman,

* Corresponding author at: Department of Psychology, Texas A&M University, 4235 TAMU, College Station, TX 77843, United States. Tel.: +1 979 845 0618; fax: +1 979 845 4727.
E-mail address: tgw@psyc.tamu.edu (T. Wilcox).

0028-3932/$ – see front matter © 2008 Elsevier Ltd. All rights reserved.
doi:10.1016/j.neuropsychologia.2008.11.014

Franceschini, & Boas, 2003; Villringer & Dirnagl, 1995). From the summated change in HbO_2 and HbR, the total change in hemoglobin (HbT) can be computed. Given that changes in HbT signal changes in regional cerebral blood flow (rCBF), having a measure of HbT is an important guide in the interpretation of NIRS data. While an increase in blood volume would result in an increase in HbO_2 and HbR, an increase in blood flow results in an increase in HbO_2 and a "washout" of HbR (i.e., an increase in relative concentration of HbO_2 and a decrease in relative concentration of HbR).

Predicting and interpreting changes in HbO_2 and HbR during cortical activation is not always straightforward, however. For example, an increase in rCBF (as indicated by HbT) produces an increase in HbO_2 and a decrease in HbR. At the same time, an increase in oxygen consumption produces a decrease in HbO_2 and an increase in HbR. Furthermore, the effect of these opposing mechanisms may be different in infants than adults (Hintz et al., 2001; Meek et al., 1998; Sakatani, Chen, Lichty, Zuo, & Wang, 1999). Hence it is important to remember that changes in relative concentrations of HbO_2 and HbR are produced by changes in blood volume, rCBF, and oxygen consumption and that the relation between these can be complex.

To capitalize on changes in HbO_2 and HbR, near-infrared light between approximately 650 and 950 nm is utilized. At these wavelengths, light is differentially absorbed by oxygenated and deoxygenated blood (Gratton, Sarno, Maclin, Corballis, & Fabiani, 2000; Villringer & Chance, 1997). Measuring the light intensity modulation during stimulus presentation, and comparing it to the light intensity during a baseline event in which no stimulus is presented, provides important information about the hemodynamic response to brain activation.

Recently, researchers have successfully applied NIRS technology to human infants in the experimental setting (e.g., Baird et al., 2002; Bortfeld, Wruck, & Boas, 2007; Pena et al., 2003; Taga, Asakawa, Maki, Konishi, & Koizumi, 2003; Wilcox, Bortfeld, Woods, Wruck, & Boas, 2005, 2008). Most of these studies have focused on region specific hemodynamic changes in the neocortex during perceptual and cognitive tasks. For example, Wilcox et al. (2005) assessed hemodynamic changes in the visual and the temporal cortex during a visual object processing task. In this task, 6.5-month-olds saw an event in which a green ball and a red box emerged successively to opposite sides of screen (Fig. 1A). Behavioral studies (Wilcox & Baillargeon, 1998a,b; Wilcox & Chapa, 2002) indicate that 4.5–11.5-month-old infants use the featural differences to interpret the event as involving two distinct objects. Analysis of the NIRS data revealed a significant increase in HbO_2 in visual and temporal cortex during the test event. Follow-up studies replicated and extended these findings to other events involving featurally distinct objects (Wilcox et al., 2008) and demonstrated that activation is observed in visual but not temporal cortex in response to control events (e.g., when the same object is seen to both sides of the screen). These data suggest that object processing is functionally localized: whereas visual cortex responds to all events involving visual objects temporal cortex responds only when the objects differ in their featural properties.

What these findings leave open to speculation, however, is the extent to which temporal cortex mediates the processing of other types of object information. For example, in adults the ventral pathway mediates processing of object features but does not typically mediate processing of the spatiotemporal properties of objects. If the ventral pathway in the infant is organized in a way similar to

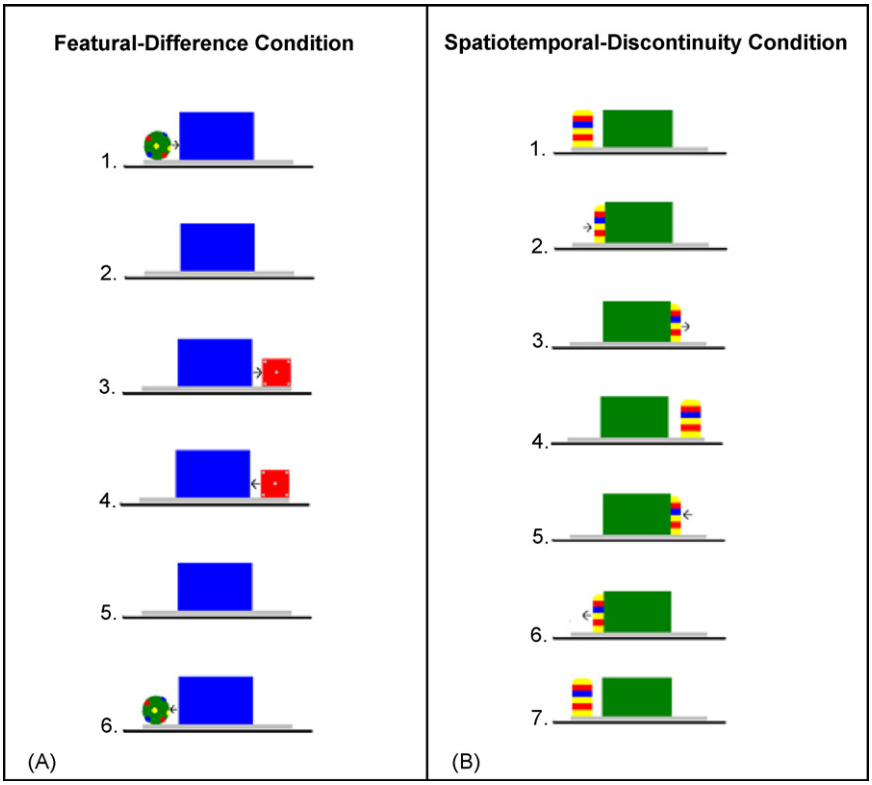

Fig. 1. The test events seen in the featural-difference (A) and spatiotemporal-discontinuity (B) condition. Although not pictured, a hand moved the objects. In the *featural-difference* condition, the ball moved right until it was fully hidden behind the occluder (2 s); the box then emerged and moved to the right edge of the platform (2 s). The box paused (1 s) and the 5 s sequence was seen in reverse. The entire 10 s ball-box cycle then repeated twice to conclude the 30 s trial. When in motion the objects moved at a rate of 12 cm/s and the occlusion interval was 1.8 s. In the *spatiotemporal-discontinuity* condition, the column moved right until it was fully occluded (2.5 s) and then the second column appeared immediately at the right edge of the occluder (the event was produced by two experimenters who had similar sized hands covered by identical white gloves) and moved right until it reached the right end of the platform (2.5 s). The column paused (1 s) and the 6 s sequence was reversed. The entire event was then repeated 1.5 times to conclude the 30 s trial. When visible, the object moved at a rate of 3 cm/s.

that of the adult, then a different pattern of activation should be observed in temporal cortex in response to events involving analysis of object features than to events involving analysis of spatiotemporal information. The present research tests this hypothesis. Infants aged 6.5 months were presented with the featural-difference event of Wilcox et al. (2005; Fig. 1A) and a spatiotemporal-discontinuity event (Fig. 1B) and NIRS data were collected. Behavioral studies have demonstrated that infants 3.5 months and older interpret the spatiotemporal-discontinuity event as involving two objects (Schweinle & Wilcox, 2004; Wilcox & Schweinle, 2003).

2. Materials and methods

2.1. Participants

Twelve 6.5-month-olds, 8 M (M age = 6 months, 15 days, range = 5 months, 12 days to 7 months, 11 days). Twelve additional infants were tested but eliminated from analysis because they failed to contribute usable NIRS data (e.g., large motion artifacts and/or poor signal-to-noise ratio). Seven infants saw the featural-difference event first.

2.2. Apparatus, stimuli, and procedure

Infants sat on a parent's lap facing a puppet-stage apparatus. The green ball used in the featural-difference event was 10.25 cm in diameter with colored dots. The red box was 10.25 cm square and decorated with silver thumbtacks. The occluder was 21.5 cm × 30 cm and made of blue cardboard. The columns used in the spatiotemporal-discontinuity event were 12 cm × 6 cm × 3 cm and made of colored Duplos. The occluder was 24 cm × 35 cm and dark green. The objects were moved by a gloved hand, which entered the apparatus through a slit in the back wall. The test events are depicted in Fig. 1.

Prior to each 30 s test trial infants were presented with a 10 s baseline (silent pause) in which a muslin-covered shade covered the front opening of the apparatus and hid the stage. The shade was raised at the beginning of each test trial and lowered at the end of each trial. Cloth-covered barriers isolated the infant from the testing room. The stage was illuminated with 20-Watt fluorescent bulbs affixed to each inside wall of the apparatus. No other lighting was used.

The time infants spent looking during each test trial was recorded by two trained observers and looking time data were time-locked to the NIRS data. Inter-observer agreement averaged 96%. A blocked design (four trials of one event followed by four trials of the other) was used because the events were produced live in the puppet-stage apparatus and each event involved different display characteristics (e.g., objects and screen). Frequent changing of display characteristics was difficult for the experimenters and distracting to the infants.

2.3. Instrumentation

The instrumentation was identical to that of Wilcox et al. (2005). Briefly, the imaging equipment contained three major components: (1) two fiber optic cables (1 mm in diameter) that delivered near-infrared light to the scalp of the participant; (2) four fiber optic cables (2.5 mm in diameter) that detected the diffusely reflected light at the scalp; and (3) an electronic control box. The electronic control box pro-

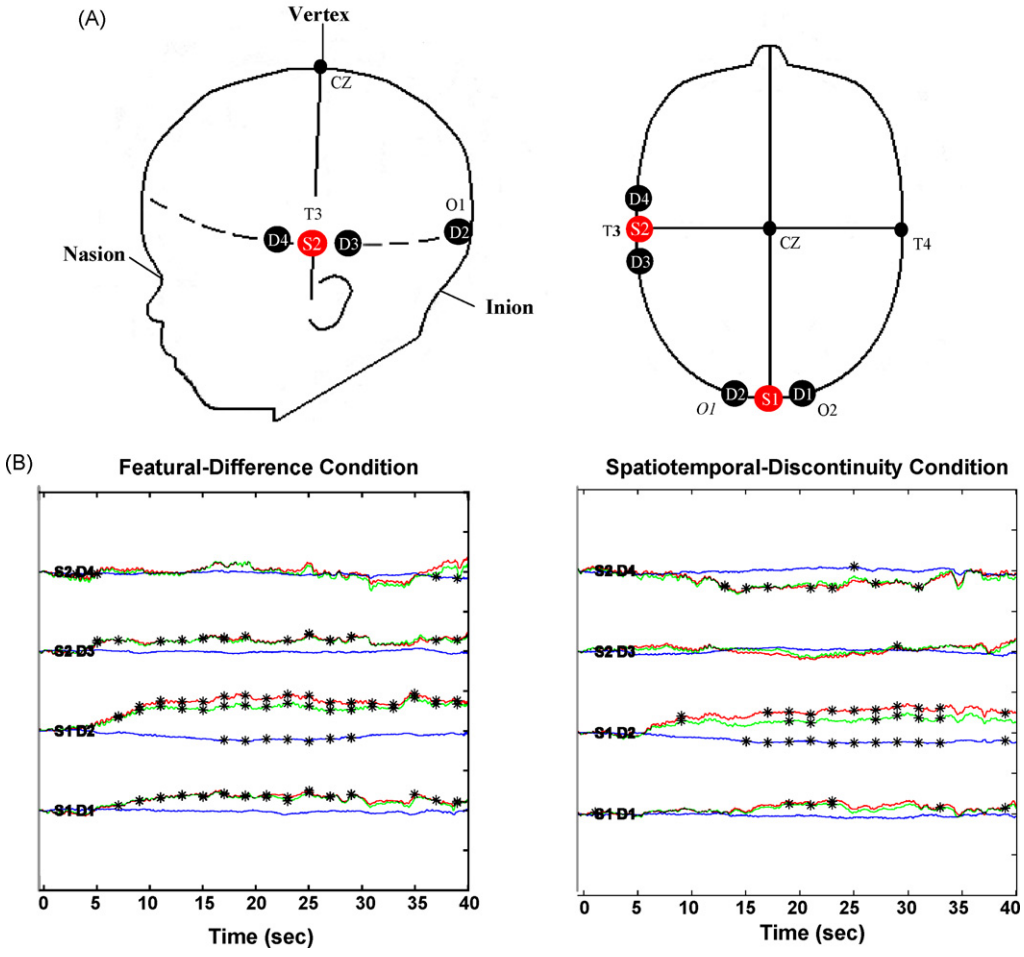

Fig. 2. Location of probe placement (A) and hemodyanmic response curves (B) for each detector. Probes were placed on the skull using the International 10–20 system. One probe was positioned so that the source (S1) lay directly above the inion and the detectors (D1 and D2) lay over the right and left visual cortex, respectively. The other source (S2) was positioned at T3 and the corresponding detectors (D3 and D4) lay anterior and posterior to T3 over temporal cortex. Emitter-detector distances were 2 cm. The hemoglobin response curves, in optical density units presented as mM × cm (*x*-axis), were averaged across participants and trials for the four detectors. For purposes of interpretation, HbT is displayed along with HbO_2 and HbR (green, red, and blue lines, respectively). The left panel of (B) displays responses obtained during the featural-discontinuity event and the right panel displays responses during the spatiotemporal-discontinuity event. The event began at time 0 and continued for 30 s; 31–40 is post-stimulus (silent pause). The asterisks indicate points along the response curves that differed significantly from 0 (baseline).

duced light at 690 and 830 nm wavelengths with two laser-emitting diodes (Boas, Franceschini, Dunn, & Strangman, 2002; TechEn Inc.). Each emitter delivered both wavelengths and each detector responded to both wavelengths. The signals received by the electronic control box were processed and relayed to a DELL Inspiron 7000™ laptop computer.

Prior to test, infants were fitted with custom-made headgear that secured the fiber optics to the scalp. The ends of the fiber optic cables were arranged in two triads, each containing one emitter and two detectors. Triad placement is shown in Fig. 2A.

2.4. Processing of the NIRS data

The NIRS data were processed, for each detector separately, using a procedure similar to that of Wilcox et al. (2005). The raw signals were acquired at the rate of 200 samples per second, digitally low-pass-filtered at 10.0 Hz, a principal components analysis was used to design a filter for systemic physiology and motion artifacts, and the data were converted to relative concentrations of oxygenated (HbO_2) and deoxygenated (HbR) blood using the modified Beer–Lambert law (Strangman, Boas, & Sutton, 2002). Changes in HbO_2 and HbR were examined using 43 s time epochs: the 3 s prior to the onset of the test event, the 30 s test event, and the 10 s following the test event. The mean optical signal from −3 to 0 s (baseline) was subtracted from the signals and other segments of the 43 s time epoch were interpreted relative to this zeroed baseline. Optical signals were averaged across trials and then infants for each condition. Trials objectively categorized as containing motion artifacts (a change in the filtered intensity greater than 5% in 1/20 s during the 3 s baseline and 30 s test event) were eliminated from the mean. A total of 11 trials (of the 96 remaining) were eliminated. Two additional trials were eliminated because the infant failed to watch the event or procedural error.

3. Results

3.1. Looking time data

The infants looked almost continuously throughout the test trials (featural-difference, $M = 27.62$, S.D. = 1.85 and speed-discontinuity, $M = 26.74$, S.D. = 1.46) suggesting that they found the test events engaging.

3.2. NIRS data

The hemoglobin concentration response curves are shown in Fig. 2. In the featural-difference condition, relative changes in HbO_2 and HbR concentration from 5 to 30 s following initiation of the event were compared to baseline. The first emergence of the box occurred at 3 s and, allowing 2 s for the hemodynamic response to become initiated, changes in HbO_2 and HbR should be detectable by 5 s. In the spatiotemporal-discontinuity condition, relative changes in HbO_2 and HbR concentration were assessed starting at 6 s (the first immediate emergence occurred at 4 s).

Three sets of analyses were conducted. First, mean HbO_2 and HbR responses for each condition and detector were compared to 0 (Table 1). In visual cortex, a significant increase in HbO_2 was obtained in response to the featural-difference event (at D1 and D2) and the spatiotemporal-discontinuity event (at D2). A significant decrease in HbR was observed at D2 in response to the spatiotemporal-discontinuity event. In temporal cortex, a significant increase in HbO_2 was observed in response to the featural-difference event at D3 but not D4. In contrast, a *decrease* in HbO_2, which approached significance ($P = .058$), was observed in response to the spatiotemporal-discontinuity event at D4 but not D3.

Second, to test the extent to which the responses observed at each detector varied by the event seen, paired sample *t*-tests were conducted for each detector with condition as the within-subjects factor (Table 1). At D1 and D2 the mean HbO_2 and HbR responses did not vary significantly by condition. However, at D3 the HbO_2 response observed in the featural-difference condition (which was positive in direction) differed from that observed in the spatiotemporal-discontinuity condition. Although the *t*-test was not statistically significant ($P = .095$), the effect size was large, Cohen's $d = .77$ (see Cohen, 1988 for evaluating effect sizes), indicating that the two groups differed in their responses. At D4, the HbO_2 response observed in the spatiotemporal-discontinuity condition (which was negative in direction) differed reliably from that observed in the featural-difference condition, and the effect size was also large, Cohen's $d = .77$.

Finally, to assess the extent to which the response observed at one detector within a neural region differed reliably from that observed at the other detector within that same region, paired-sample *t*-tests were conducted for each neural region and condition

Table 1
Relative change in HbO_2 and HbR concentration displayed by detector and condition.

Neural Region	Detector	Chromophore	Condition		Paired *t*-tests
			Featural-difference *M* (S.D.)	Spatiotemporal-discontinuity *M* (S.D.)	
Visual	D1	HbO_2	0.0066 (.006)** $t = 3.96$, d.f. = 11	0.0035 (.011) $t = 1.10$, d.f. = 11	$t = -1.01$, d.f. = 11
		HbR	−0.0003 (.003) $t = -0.35$, d.f. = 11	−0.0009 (.005) $t = -0.61$, d.f. = 11	$t = -0.40$, d.f. = 11
	D2	HbO_2	0.0143 (.018)** $t = 2.79$, d.f. = 11	0.0092 (.014)* $t = 2.21$, d.f. = 11	$t = -1.11$, d.f. = 11
		HbR	−0.0035 (.006) $t = -2.03$, d.f. = 11	−0.0038 (.006)* $t = -2.23$, d.f. = 11	$t = -0.26$, d.f. = 11
Temporal	D3	HbO_2	0.0058 (.009)** $t = 2.34$, d.f. = 11	−0.0001 (.006) $t = -0.08$, d.f. = 10	$t = -1.84$, d.f. = 10+
		HbR	−0.0004 (.003) $t = -0.35$, d.f. = 11	0.0007 (.004) $t = 0.51$, d.f. = 10	$t = 0.74$, d.f. = 10
	D4	HbO_2	0.0010 (.009) $t = 0.39$, d.f. = 10	−0.0063 (.010) $t = -2.14$, d.f. = 10	$t = -2.47$, d.f. = 10*
		HbR	−0.0008 (.003) $t = -0.94$, d.f. = 10	0.0001 (.003) $t = 0.18$, d.f. = 10	$t = -0.69$, d.f. = 10

Note: Cells contain mean relative optical density units in mM x cm averaged from 5 to 30 s (featural-difference condition) and 6 to 30 s (spatiotemporal-discontinuity condition). Mean responses were compared to 0 using *t*-tests (two-tailed) and the asterisks indicate those responses that differed significantly from 0 (*$P < .05$ and **$P < .025$). The last column contains paired *t*-tests (two-tailed) comparing responses across condition (*$P < .05$ and +$P < .1$ with a large effect size). Effect sizes are reported in the text.

Table 2
Comparison of hemodynamic responses across detectors within each neural region.

Condition	Chromophore	Visual cortex D1 vs. D2	Temporal cortex D3 vs. D4
Featural-difference	HbO_2	$t = -1.41$, d.f. = 11	$t = 2.32$, d.f. = 10*
	HbR	$t = 1.45$, d.f. = 11	$t = 0.28$, d.f. = 10
Spatiotemporal-discontinuity	HbO_2	$t = -1.30$, d.f. = 11	$t = 2.19$, d.f. = 9+
	HbR	$t = 1.69$, d.f. = 11	$t = 0.55$, d.f. = 9

Note: Paired *t*-tests compared hemodynamic responses, for each condition and chromophore, across detectors within each neural region. The symbols indicate the comparison in which the responses observed at the two detectors differed reliably from each other using two-tailed statistics (*$P < .05$ and +$P < .1$ with a large effect size). Effect sizes are reported in the text.

with detector as the within-subjects factor (Table 2). In visual cortex, hemodynamic responses did not vary significantly by detector, for infants in either condition. In temporal cortex, some differences emerged. In the featural-difference condition, the HbO_2 response observed at D3 differed significantly from that observed at D4, Cohen's $d = .53$. In the spatiotemporal-discontinuity condition, the HbO_2 response observed at D3 and D4 also differed. Although the t-test was not statistically significant ($P = .056$) the effect size was large, Cohen's $d = .75$.

4. Discussion

The present research used near-infrared spectroscopy to assess neural activation, as measured by changes in blood volume and oxygenation, in visual and temporal cortex in 6.5-month-olds during two object processing tasks, one that involved analysis of object features and the other that required analysis of spatiotemporal information.

As predicted, a hemodynamic response was observed in visual cortex (D1 and D2) in both conditions and the responses did not vary significantly by condition. At the same time, the hemodynamic response obtained at D1 differed qualitatively from that obtained at D2. For example, a significant increase in HbO_2 was observed at D2 in response to both events and a significant decrease in HbR was observed at D2 in response to the featural-difference event. In comparison, a less robust response was observed at D1: a significant increase in HbO_2 was observed in response to the featural-difference event only and no significant decreases in HbR were observed. Why were qualitatively different hemodynamic response patterns observed at D1 and D2? Recall that in the present study the light source was placed directly above the inion, so that D1 lay over the left visual cortex whereas D2 lay over the right visual cortex. One possible explanation is that in the infant, the left and right visual cortices are organized slightly differently, so that structurally analogous areas in the two hemispheres respond differently to the same visual stimuli. Different functional responses could lead to different hemodynamic responses. Alternatively, it is possible that the two hemispheres are not structurally identical, so that measuring from skull locations equidistant from the midline, but in different hemispheres, does not guarantee measurements from structurally (let alone functionally) analogous neural areas. A final possibility is that these results reflect an asymmetry in the degree of neurovascular regulation in visual areas of the two hemispheres. That is, in right visual cortex changes in rCBF may not be as well matched to energy demands (oxygen consumption) as in left visual cortex. Additional research will be needed to (a) establish the extent to which reliable hemispheric differences in hemodynamic responses to visual stimuli exist in V and other areas and (b) identify the basis of these differences. In the meantime, the patterns observed in the present experiment are best interpreted with caution.

As predicted, the hemodynamic response observed in temporal cortex differed by condition, although the way in which this was manifested was unexpected. A significant *increase* in HbO_2 was observed at D3 in the featural-difference condition and a *decrease* in HbO_2 was observed at D4 in the spatiotemporal-discontinuity condition. In addition, the responses observed at each detector differed by condition, and within condition the responses differed by detector. These dissociations suggest that the cortical regions directly anterior to and posterior to T3 are functionally distinct.

On the basis of neuroanatomical data obtained with human infants (Conel, 1939–1967; Purpura, 1975) and on data demonstrating the relation between 10 and 20 skull coordinates and underlying neural structure in adults (Okamoto et al., 2004), we suspect that the area posterior to T3 lies near the temporal–occipital border and may include part of the lateral occipital cortex (LOC). Neuroimaging data obtained with adults (Grill-Spector et al., 1998, 1999, 2001; Haxby et al., 1991; Kourtzi & Kanwisher, 2001; Kraut et al., 1997; Malach et al., 1995) indicate that the LOC is involved in the processing of object features, but does not respond to the spatiotemporal properties of objects. In contrast, we suspect that the area anterior to T3 lies close to the medial or superior temporal gyrus. This area does not appear to mediate processing of featural differences or spatiotemporal discontinuities, at least in the infant.

Unexpectedly, a *decrease* in HbO_2 was observed at D4 in the spatiotemporal-discontinuity condition, and this response differed significantly from the response obtained in the featural-difference condition. In addition, there was a decrease in HbT indicating a decrease in rCBF. One possible explanation for this unusual pattern of results is that viewing the spatiotemporal-discontinuity event led to neural deactivation and a corresponding decrease in rCBF and blood volume. Either of these could have produced an increase in the local concentration of HbR relative to HbO_2. Another, more likely explanation, assumes no activation at D4. The decrease in HbO_2 reflects, instead, the blood supply being diverted to nearby areas that are active. These areas could lie either deeper in the cortex or adjacent on the surface (e.g., areas associated with the dorsal system). Regardless of how to best conceptualize the hemodynamic response obtained at D4 during the spatiotemporal-discontinuity event, it is important to remember that this response differed from that observed at D3 during the spatiotemporal-discontinuity event, suggesting that the neural regions from which these two detectors were measuring differ in their functional response to the event and/or in the nature of their neurovascular regulatory mechanisms.

The data also suggest that HbO_2 is a more robust measure of the hemodynamic response than HbR. A significant increase in HbO_2 was observed at a number of detectors, in both V and T, and in response to both the featural-difference and spatiotemporal-discontinuity events. In contrast, the only detector at which we saw a significant decrease in HbR and a corresponding increase in HbO_2 was at D2 in V (spatiotemporal-discontinuity condition). These results are consistent with those of other investigators who have reported that, generally speaking, HbO_2 is a more robust and reliable measure of neural activation than HbR (Bartocci et al., 2000; Chen et al., 2002; Hoshi & Tamura, 1993; Jasdzewski et al., 2003; Kato, Kamei, Takashima, & Ozaki, 1993; Sakatani et al., 1999; Strangman et al., 2002, 2003).

Finally, the hemodynamic responses observed in temporal cortex appeared smaller in magnitude and less robust than those observed in visual cortex. For example, the magnitude of the response observed at D3 in response to the featural-difference event was less than that observed at D2. Although we can only speculate, the less robust responses observed at D3 and D4 may reflect greater immaturity of the temporal as compared to visual cortex. This would be consistent with neuroanatomical and metabolic data (Chugani & Phelps, 1986; Conel, 1939–1967; Franceschini et al., 2007; Purpura, 1975) and might reflect less efficient neural processing and/or energy demands associated with maturational events.

In summary, the present results demonstrate that there are region specific differences in visual object processing in human infants and that NIRS is sufficiently sensitive to detect these differences. The ability to study functional brain activation in awake, processing infants represents a significant advancement in the field of developmental neuroscience and will allow investigators to study localized functional maturation of the human brain.

Acknowledgements

This research was supported by grants from the National Institutes of Health (HD48943 to T.W., HD46533 to H.B., and P41-RR14075 to D.B.). We would like to thank Tracy Smith and the

undergraduate assistants in the Infant Cognition Laboratory at Texas A&M University for their help with data collection and the parents who so graciously agreed to have their infants participate in the research.

References

Bachevalier, J., Brickson, M., Hagger, C., & Mishkin, M. (1990). Age and sex differences in the effects of selective temporal lobe lesion on the formation of visual discrimination habits in rhesus monkeys (*Macaca mulatta*). *Behavioral Neuroscience*, *104*, 885–899.

Baird, A. A., Kagan, J., Gaudette, T., Walz, K. A., Hershlag, N., & Boas, D. A. (2002). Frontal lobe activation during object permanence: Data from near-infrared spectroscopy. *NeuroImage*, *16*, 1120–1126.

Bartocci, M., Winberg, J., Ruggiero, C., Bergqvist, L. L., Serra, G., & Lagercrantz, H. (2000). Activation of olfactory cortex in newborn infants after odor stimulation: A functional near-infrared spectroscopy study. *Pediatric Research*, *48*, 18–23.

Bly, B. M., & Kosslyn, S. M. (1997). Functional anatomy of object recognition in humans: Evidence from positron emission tomography and functional magnetic resonance imaging. *Current Opinion in Neurology*, *10*, 5–9.

Boas, D. A., Franceschini, M. A., Dunn, A. K., & Strangman, G. (2002). Noninvasive imaging of cerebral activation with diffuse optical tomography. In R. D. Frostig (Ed.), *Vivo optical imaging of brain function* (pp. 193–221). Boca Raton: CRC Press.

Bortfeld, H., Wruck, E., & Boas, D. A. (2007). Assessing infants' cortical response to speech using near-infrared spectroscopy. *Neuroimage*, *34*, 407–415.

Braddick, O., & Atkinson, J. (2007). Development of brain mechanisms for visual global processing and object segmentation. In C. von Hofsten & K. Rosander (Eds.), From action to cognition (Progress in Brain Research, vol. 164) (pp. 151–168). Amsterdam: Elsevier.

Braddick, O., Atkinson, J., & Wattam-Bell, J. (2003). Normal and anomalous development of visual motion processing: Motion coherence and 'orsal-stream vulnerability'. *Neuropsychologia*, *41*(13), 1768–1783.

Chugani, H., & Phelps, M. (1986). Maturational changes in cerebral function in infants determined by 18FDG positron emission tomography. *Science*, *231*, 840–843.

Cohen, J. (1988). *Statistical power analysis for the behavioral sciences*. Hillsdale, NJ: Lawrence Earlbaum Associates.

Conel, J. L. (1939–1967). *The postnatal development of the human cerebral cortex* Cambridge, MA: Harvard University Press.

De Haan, M., & Nelson, C. (1999). Brain activity differentiates face and object processing in 6-month-old infants. *Developmental Psychology*, *35*, 1113–1121.

De Yoe, E. A., & Van Essen, D. C. (1988). Concurrent processing streams in monkey visual cortex. *Trends in Neurosciences*, *11*, 219–226.

Franceschini, M. A., Thaker, S., Themelis, G., Krishnamoorthy, K. K., Bortfeld, H., Diamond, S. G., Boas, D. A., Arvin, K., & Grant, P. E. (2007). Assessment of infant brain development with frequency-domain near-infrared spectroscopy. *Pediatric Research*, *61*, 546–551.

Goodale, M. A., & Milner, A. D. (1992). Separate visual pathways for perception and action. *Trends in Neurosciences*, *15*, 20–25.

Gratton, G., Sarno, A., Maclin, E., Corballis, P. M., & Fabiani, M. (2000). Toward noninvasive 3-D imaging of the time course of cortical activity: Investigation of the depth of the event-related optical signal. *NeuroImage*, *11*, 491–504.

Grill-Spector, K., Kourtzi, Z., & Kanwisher, N. (2001). The lateral occipital complex and its role in object recognition. *Vision Research*, *41*, 1409–1422.

Grill-Spector, K., Kushnir, T., Hendler, T., Edelman, S., Itzchak, Y., & Malach, R. (1998). A sequence of object-processing stages revealed by fMRI in the human occipital lobe. *Human Brain Mapping*, *6*, 316–328.

Grill-Spector, K., Kushnir, T., Edelman, S., Avidan, G., Itzchak, Y., & Malach, R. (1999). Differential processing of objects under various viewing conditions in the human lateral occipital complex. *Neuron*, *24*, 187–203.

Gunn, A., Cory, E., Atkinson, J. A., Braddick, O., Wattam-Bell, J., Guzzetta, A., & Cioni, G. (2002). Dorsal and ventral stream sensitivity in normal development and hemiplegia. *Neuroreport*, *13*(6), 843–847.

Haxby, J. V., Grady, C. L., Horwitz, B., Ungerleider, L. G., Mishkin, M., Carson, R. E., et al. (1991). Dissociation of object and spatial visual processing pathways in human extrastriate cortex. *Proceedings of the National Academy of Sciences*, *88*, 1621–1625.

Hoshi, Y., & Tamura, M. (1993). Dynamic multichannel near-infrared optical imaging of human brain activity. *Journal of Applied Physiology*, *75*, 1842–1846.

Hintz, S. R., Benaron, D. A., Siegel, A. M., Zourabian, A., Stevenson, D. K., & Boas, D. A. (2001). Bedside functional imaging of the premature infant brain during passive motor activation. *Journal of Perinatal Medicine*, *29*, 335–343.

Jasdzewski, G., Strangman, G., Wagner, J., Kwong, K. K., Poldrack, R. A., & Boas, D. A. (2003). Differences in the hemodynamic response to event-related motor and visual paradigms as measured by near-infrared spectroscopy. *NeuroImage*, *20*, 479–488.

Kato, T., Kamei, A., Takashima, S., & Ozaki, T. (1993). Human visual cortical function during photic stimulation monitoring by means of near-infrared spectroscopy. *Journal of Cerebral Blood Flow and Metabolism*, *13*, 516–520.

Kourtzi, Z., & Kanwisher, N. (2001). Representation of perceived object shape by the human lateral occipital complex. *Science*, *293*, 1506–1509.

Kraut, M., Hart, J., Soher, B. J., & Gordon, B. (1997). Object shape processing in the visual system evaluated using functional MRI. *Neurology*, *48*, 1416–1420.

Livingstone, M., & Hubel, D. (1988). Segregation of form, color, movement, and depth: Anatomy, physiology, and perception. *Science*, *240*, 740–749.

Malach, R., Reppas, J. B., Benson, R. R., Kwong, K. K., Jiang, H., Kennedy, W. A., Ledden, P. J., Brady, T. J., Rosen, B. R., & Tootell, R. B. H. (1995). Object-related activity revealed by functional magnetic resonance imaging in human occipital cortex. *Proceedings of the National Academy of Sciences*, *92*, 8135–8139.

Meek, J. H., Firbank, M., Elwell, C. E., Atkinson, J., Braddick, O., & Wyatt, J. S. (1998). Regional hemodynamic responses to visual stimulation in awake infants. *Pediatric Research*, *43*, 840–843.

Mishkin, M., Ungerleider, L. G., & Macko, K. A. (1983). Object vision and spatial vision: two cortical pathways. *Trends in Neuroscience*, *6*, 414–417.

Obrig, H., Wolf, T., Döge, C., Hülsing, J. J., Dirnagl, U., & Villringer, A. (1996). Cerebral oxygen changes during motor and somatosensory stimulation in humans, as measured by near-infrared spectroscopy. *Advances in Experimental Medicine and Biology*, *388*, 219–224.

Okamoto, M., Dan, H., Sakamoto, K., Takeo, K., Shimizu, K., Kohno, S., et al. (2004). Three-dimensional probabilistic anatomical cranio-cerebral correlation via the international 10-20 system oriented for transcranial functional brain mapping. *Neuroimage*, *21*, 99–111.

Orban, G. A., Van Essen, D., & Fanduffel, W. (2004). Comparative mapping of higher visual areas in monkeys and humans. *Trends in Cognitive Sciences*, *8*, 315–324.

Pena, M., Maki, A., Kovacic, D., Dehaene-Lambertz, G., Koizumi, H., Bouquet, F., & Mehler, J. (2003). Sounds and silence: An optical topography study of language recognition at birth. *Proceedings of the National Academy of Sciences*, *100*, 11702–11705.

Purpura, D. (1975). Dendritic differentiation in the human cerebral cortex: Normal and aberrant developmental patterns. *Advances in Neurology*, *12*, 91–100.

Rodman, H. R., Skelly, J. P., & Gross, C. G. (1991). Stimulus selectivity and state dependence of activity in inferior temporal cortex in infants monkeys. *Proceedings of the National Academy of Sciences*, *88*, 7572–7575.

Sakatani, K., Chen, S., Lichty, W., Zuo, H., & Wang, Y. (1999). Cerebral blood oxygenation changes induced by auditory stimulation in newborn infants measured by near infrared spectroscopy. *Early Human Development*, *55*, 229–236.

Schweinle, A., & Wilcox, T. (2004). Sex differences in infants' ability to represent complex event sequences. *Infancy*, *6*, 333–359.

Strangman, G., Boas, D. A., & Sutton, J. P. (2002). Non-invasive neuroimaging using near-infrared light. *Biological Psychiatry*, *52*, 679–693.

Strangman, G., Franceschini, M. A., & Boas, D. A. (2003). Factors affecting the accuracy of near-infrared spectroscopy concentration calculations for focal changes in oxygenation parameters. *NeuroImage*, *18*, 865–879.

Taga, G., Asakawa, K., Maki, A., Konishi, Y., & Koizumi, H. (2003). Brain imaging in awake infants by near-infrared optical topography. *Proceedings of the National Academy of Sciences*, *100*, 10722–10727.

Tanaka, K. (2000). Mechanisms of visual object recognition studied in monkeys. *Spatial Vision*, *13*, 147–163.

Tootell, R. B. H., Tsao, D., & Vanduffel, W. (2003). Neuroimaging weighs in: Humans meet macaques in "primate" visual cortex. *The Journal of Neuroscience*, *23*, 3981–3989.

Tsunoda, K., Yamane, Y., Nishizaki, M., & Tanifuji, M. (2001). Complex objects are represented in macaque inferotemporal cortex by the combination of feature columns. *Nature Neuroscience*, *4*, 832–838.

Ungerleider, L. G., & Mishkin, M. (1982). Two cortical visual systems. In D. J. Ingle, M. A. Goodale, & R. J. W. Mansfield (Eds.), *Analysis of visual behavior* (2nd ed., vol. 1–8, pp. 549–586). Cambridge, MA: MIT Press.

Villringer, A., & Chance, B. (1997). Non-invasive optical spectroscopy and imaging of human brain function. *Trends in Neuroscience*, *20*, 435–442.

Villringer, A., & Dirnagl, U. (1995). Coupling of brain activity and cerebral blood flow: Basis of functional imaging. *Cerebrovascular and Brain Metabolism Reviews*, *7*, 240–276.

Wang, G., Tanaka, K., & Tanifuji, M. (1996). Optical imaging of functional organization in the monkey inferotemporal cortex. *Science*, *272*, 1665–1668.

Wang, G., Tanifuji, & Tanaka, K. (1998). Functional architecture in monkey inferotemporal cortex revealed by in vivo optical imaging. *Neuroscience Research*, *31*, 33–46.

Webster, M. J., Ungerleider, L. G., & Bachevalier, J. (1991). Connections of inferior temporal areas TE and TEO with medial temporal-lobe structures in infant and adult monkeys. *Journal of Neuroscience*, *11*, 1095–1116.

Webster, M. J., Ungerleider, L. G., & Bachevalier, J. (1995). Development and plasticity of the neural circuitry underlying visual recognition memory. *Canadian Journal of Physiological Pharmacology*, *73*, 1364–1371.

Wilcox, T., & Baillargeon, R. (1998a). Object individuation in infancy: The use of featural information in reasoning about occlusion events. *Cognitive Psychology*, *37*, 97–155.

Wilcox, T., & Baillargeon, R. (1998b). Object Individuation in young infants: Further evidence with an event monitoring task. *Developmental Science*, *1*, 127–142.

Wilcox, T., Bortfeld, H., Woods, R., Wruck, E., & Boas, D. A. (2005). Using near-infrared spectroscopy to assess neural activation during object processing in infants. *Journal of Biomedical Optics*, *10*, 1–9.

Wilcox, T., Bortfeld, H., Woods, R., Wruck, E., & Boas, D. (2008). Hemodynamic response to featural changes in the occipital and inferior temporal cortex in infants: A preliminary methodological exploration. *Developmental Science*, *11*, 361–370.

Wilcox, T., & Chapa, C. (2002). Infants' reasoning about opaque and transparent occluders in an individuation task. *Cognition*, *85*, B1–B10.

Wilcox, T., & Schweinle, A. (2003). Infants' use of speed information to individuate objects in occlusion events. *Infant Behavior and Development*, *26*, 253–282.